EPSC Abstracts
Vol. 13, EPSC-DPS2019-1910-2, 2019
EPSC-DPS Joint Meeting 2019

EPSC
EPSC-DPS Joint Meeting 2019
15–20 September 2019 | Geneva, Switzerland

Rock Size Distributions at the InSight Landing Site

C. Charalambous[1], M. Golombek[2], T. Pike[1], N. H. Warner[3], V. Ansan[4], E. Hauber[5], C. Weitz[6], J. Grant[7], N. Williams[2], S. Wilson[7], A. DeMott[3], M. Kopp[3], H. Lethcoe[2]. [1]Imperial College, London, Department of Electrical and Electronic Engineering, UK [2]Jet Propulsion Laboratory, California Institute of Technology, Pasadena, CA, USA, [3]SUNY Geneseo, NY, USA, [4]University of Nantes, Laboratory of Planetary and Geodynamics, France, [5]German Aerospace Center (DLR), Berlin, Germany [6]Planetary Science Institute, Arlington, VA, USA [7]Center for Earth and Planetary Studies, National Air and Space Museum, Smithsonian Institution, Washington, USA.

Introduction: The Discovery mission InSight (Interior Exploration using Seismic Investigations, Geodesy and Heat Transport) successfully landed in western Elysium Planitia on November 26, 2018. Dedicated to the study of the martian interior, the lander is located at 4.502°N/135.623°E (planetocentric coordinates) within a quasi-circular, shallow depression informally named Homestead hollow [1]. This is a heavily modified and degraded crater, with a smooth surface. Rock populations near the lander are mostly pebble sized with few larger rocks. Beyond the hollow, more cobble and boulder size rocks are present.

In this work, we analyze the rock abundance and variability nearby the lander by using images from both the lander-mounted Instrument Context Camera (ICC) and the robotic arm-mounted Instrument Deployment Camera (IDC).

Measurements: Measuring rocks in the workspace of InSight was required to successfully deploy the instruments, which have requirements that the locations be free of 3 cm high rocks. Rock counts were measured multiple times by more than one person to check for consistency. Measurements were done separately through ArcGIS by fitting convex hulls and ImageJ by fitting ellipses. The diameter was taken as the average of the two horizontal axes.

Four areas were identified for characterizing rock abundances (Figs. 1 and 2): 1) a high rock abundance area to the west of the workspace, 2) the low rock abundance workspace area, 3) instrument footprints, and 4) the far-field radiometer (RAD) spot on the rougher and rockier terrain to the lander's northwest.

Size-Frequency Distributions: The cumulative fractional area (CFA) covered by rocks versus diameter is shown in Fig. 3. In the main workspace area and its near vicinity, the distribution of rocks 2-8 cm diameter follows a 1% rock abundance for exponential rock size-frequency models that have been used to describe rock populations for landing spacecraft [4, 5].

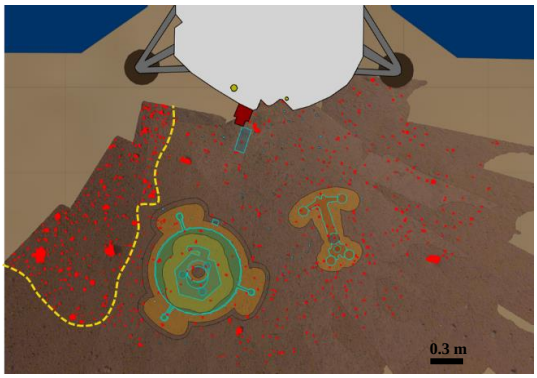

Figure 1. InSight WebGIS image of workspace near the lander (top) showing the seismometer (left) and heat flow probe (right). The yellow dashed line indicates boundary between the high rock abundance area to the west of the workspace and the smooth plains. Show in red are rocks larger than 1 cm.

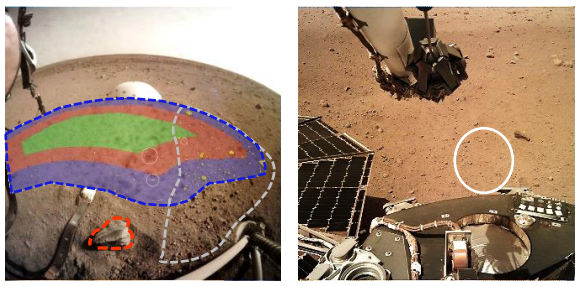

Figure 2. (Left) The workspace area within the reach of the robotic arm (blue), the higher abundance area (grey) and the turtle rock (red) as the largest rock in the near vicinity of the workspace (Right) The far-field radiometer (RAD) spot is circled in white.

Measurements of the largest rocks nearby the lander including five of at the edge of the workspace yields a CFA close to an exponential model rock abundance of 1% for rocks 10-20 cm diameter. At diameters below 4 cm, the CFA of the high rock abundance area increases steeply approaching 9% CFA for rocks >1 cm. This region represents a transition to

the rockier field to the west of the lander. The far RAD spot has higher rock abundance with a CFA between 2% and 5% for diameters of 4-10 cm. The CFA of the largest rocks measured is most similar to the Phoenix landing site (2%). The steep increase in area covered by rocks less than 4 cm most closely resembles clast counts on the Gusev cratered plains from Spirit [4] and the Phoenix landing site [5].

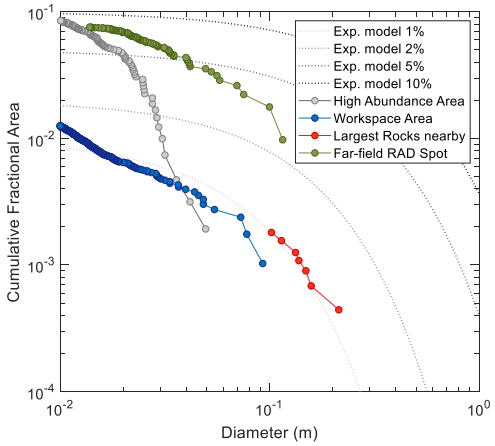

Figure 3 Cumulative Fractional Area of rocks versus diameter of the different areas in the near vicinity of the high-resolution mosaic. Dotted lines: 1%, 2%, 5% and 10% exponential models [6].

The equivalent plot in cumulative number of rocks per square meter versus diameter is shown in Fig. 4. The workspace distribution and largest rocks nearby the lander are parallel but less than an exponential model of rock abundance of 1% for diameters of less than 4 cm. These distributions rise more steeply at smaller diameters with a greater slope than the models and resemble clast counts on the Gusev cratered plains [4]. For pebbles <2 cm, the workspace area exhibits even steeper slopes as seen in the individual clast counts within the instrument footprints in Fig. 5. Taken together, these rock distributions and CFAs are most similar to the ~2% CFA measured at the Phoenix landing site [5] and below the 5% CFA measured at the Spirit landing site [4] for diameters >10 cm.

Discussion: The overall measurements above are consistent with expectations from average rock statistics of the entire landing E9 ellipse (130 km by 27 km) [2]. The low rock abundance within the hollow is due to the dearth of rocks larger than 10 cm. The lack of large rocks in the hollow is likely due to the sand that was deposited in the crater as it degraded [7]. The higher abundance area to the west of the workspace is transitional to a rockier field to the west of the lander [7], possibly mixed with the disturbed field of duricrust fragments [8].

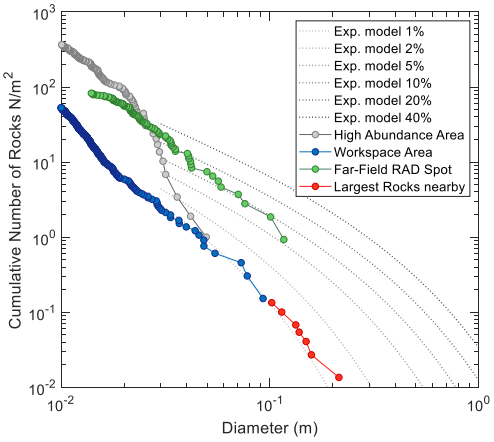

Figure 4 Cumulative number of rocks versus diameter per square meter with 1%, 2%, 5%, 10%, 20% and 40% exponential models cropped at 3 cm.

The very low rock abundance and highly steep slopes of the rock distributions together indicate a surface with very low rock abundance that is dominated by sand-sized material, consistent with orbital [1] and lander radiometer [10] thermal inertia measurements [2].

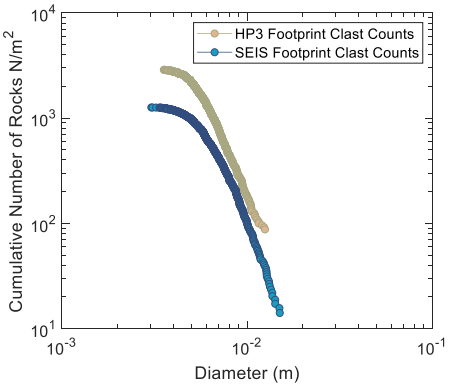

Figure 5 Cumulative number of rocks per meter squared versus diameter of clast observations within each instrument's footprint area [7].

References: [1] Parker, T. *et al*. (2019) 50th LPSC. [2] Golombek, M., *et al*. (2017) *SSR*, 211, 5-95. [3] Hartman, W. (2005) *Icarus* 174, 294–320. [4] Golombek *et al*. (2006) *JGR*, 211. [5] Golombek *et al*., (2012), *Mars* 7, 1-22. [6] Weitz *et al*. (2019) 50th LPSC. [7] Warner *et al*. (2019) 50th LPSC. [8] Ansan *et al*. (2019), 50th LPSC. [9] Golombek et al. (2018) 49th *LPSC*, #2319.[10] Mueller et al., this issue.